Hypertension Research (2020) 43:281–295
https://doi.org/10.1038/s41440-019-0374-8

ARTICLE

Brain angiotensin type-1 and type-2 receptors: cellular locations under normal and hypertensive conditions

Colin Sumners[1] · Amy Alleyne[2] · Vermalí Rodríguez[1] · David J. Pioquinto[2] · Jacob A. Ludin[2] · Shormista Kar[1] · Zachary Winder[1,2] · Yuma Ortiz[2] · Meng Liu[1] · Eric G. Krause[2] · Annette D. de Kloet[1]

Received: 24 June 2019 / Revised: 25 October 2019 / Accepted: 2 November 2019 / Published online: 18 December 2019

Abstract

Brain angiotensin-II (Ang-II) type-1 receptors (AT1Rs), which exert profound effects on normal cardiovascular, fluid, and metabolic homeostasis, are overactivated in and contribute to chronic sympathoexcitation and hypertension. Accumulating evidence indicates that the activation of Ang-II type-2 receptors (AT2Rs) in the brain exerts effects that are opposite to those of AT1Rs, lowering blood pressure, and reducing hypertension. Thus, it would be interesting to understand the relative cellular localization of AT1R and AT2R in the brain under normal conditions and whether this localization changes during hypertension. Here, we developed a novel AT1aR-tdTomato reporter mouse strain in which the location of brain AT1aR was largely consistent with that determined in the previous studies. This AT1aR-tdTomato reporter mouse strain was crossed with our previously described AT2R-eGFP reporter mouse strain to yield a novel dual AT1aR/AT2R reporter mouse strain, which allowed us to determine that AT1aR and AT2R are primarily localized to different populations of neurons in brain regions controlling cardiovascular, fluid, and metabolic homeostasis. Using the individual AT1aR-tdTomato reporter mice, we also demonstrated that during hypertension induced by the administration of deoxycorticosterone acetate-salt, there was no shift in the expression of AT1aR from neurons to microglia or astrocytes in the paraventricular nucleus, a brain area important for sympathetic regulation. Using AT2R-eGFP reporter mice under similar hypertensive conditions, we demonstrated that the same was true of AT2R expression in the nucleus of the solitary tract (NTS), an area critical for baroreflex control. Collectively, these findings provided a novel means to assess the colocalization of AT1R and AT2R in the brain and a novel view of their cellular localization in hypertension.

Keywords Renin-angiotensin system · Neurogenic hypertension · Blood pressure · Transgenic reporter mice

Introduction

The renin-angiotensin system (RAS) plays a fundamental role in body fluid and cardiovascular homeostasis under normal physiological conditions [1–3]. An important aspect of RAS-mediated actions is the central nervous system (CNS)-mediated stimulatory effects of angiotensin-II (Ang-II) on the Ang-II type-1 receptor (AT1R), which augments thirst, sympathetic nerve activity and vasopressin secretion [4–6]. Importantly, the AT1R-mediated effects of Ang-II within the CNS are exacerbated in and contribute to the chronic sympathoexcitation that underlies resistant or "neurogenic" hypertension [7–9]. Consistent with these effects of Ang-II under physiological and pathological conditions, AT1Rs are located in brain areas and nuclei that control blood pressure and fluid balance, as demonstrated by the use of receptor autoradiography, radioactive in situ hybridization, and transgenic reporter mice [10–15]. In addition to AT1Rs, the brain clearly contains angiotensin type-2 receptors (AT2Rs) [10–12, 16]. While the brain localization of AT2R differs from that of AT1R *in general*, it is evident that AT2Rs are found within or adjacent to

Supplementary information The online version of this article (https://doi.org/10.1038/s41440-019-0374-8) contains supplementary material, which is available to authorized users.

✉ Annette D. de Kloet
adekloet@ufl.edu

[1] Department of Physiology and Functional Genomics, College of Medicine, University of Florida, Gainesville, FL 32611, USA

[2] Department of Pharmacodynamics, College of Pharmacy, University of Florida, Gainesville, FL 32611, USA

CNS areas/nuclei that contain AT1Rs and are involved in cardiovascular regulation, including the nucleus of the solitary tract (NTS), rostral ventrolateral medulla (RVLM), and paraventricular nucleus (PVN) of the hypothalamus. This particular localization of AT2Rs in or around cardiovascular control centers is consistent with previous studies and the emerging view that their activation has blood pressure-lowering and antihypertensive effects, possibly via a reduction in sympathetic outflow, i.e., effects that are fundamentally opposite to those of AT1R activation [17–29].

Considering these findings, it would be of interest to determine the relative cellular localization of AT1R and AT2R within cardiovascular control centers of the brain to ultimately help to determine whether the opposite cardiovascular effects mediated by these receptors are due to opposing effects on the same cells or the modulation of different or interrelated neuronal circuits. Furthermore, it is apparent that the prohypertensive actions of AT1R involve the stimulation of proinflammatory mechanisms in the brain and that the antihypertensive actions mediated by brain AT2R involve the induction of anti-inflammatory mechanisms [18, 30–32]. Thus, it would be of interest to determine whether the resident inflammatory cells of the CNS, microglia, and astrocytes [33, 34], express AT1R and AT2R within cardiovascular control centers under baseline conditions and whether this expression changes during neurogenic hypertension.

To address these issues, we first developed two novel genetically modified mouse strains as follows: (1) We used the Cre-loxP system to develop a novel AT1aR reporter mouse strain to visualize the cellular localization of AT1aR in the brain and (2) we crossed this AT1aR reporter mouse strain with our previously reported AT2R-eGFP reporter mouse strain [16, 35] to develop a novel dual AT1aR/AT2R reporter mouse strain; this allowed us to visualize the locations of both receptors at the same time.

Male and female dual AT1aR/AT2R mice were used to determine the relative cellular distributions of these receptors in brain regions involved in cardiovascular control and fluid balance. The AT1aR and AT2R-eGFP single-reporter mice were used to determine whether the cellular distribution (neurons vs. microglia vs. astrocytes) of these receptors were altered under conditions of established neurogenic hypertension induced by the administration of deoxycorticosterone acetate (DOCA) and salt. In these latter studies, to locate AT1aR, we focused on the PVN, a brain area containing high levels of this angiotensin receptor subtype that is of major importance in sympathetic regulation. For studies on AT2R, we focused on the NTS, an area that is of major importance in baroreflex control and sympathetic outflow and the major site of the expression of this receptor subtype among brain cardiovascular control centers.

Materials and methods

Animals

Mice

Mice were on a C57BL/6J background. The three following genetic mouse models were used to identify cells that contained AT1aR and/or AT2R in this study:

(1) AT1aR-tdTomato reporter mice: AT1aR-Cre-Zsgreen knock-in mice were generated by the University of Florida and Biocytogen LLC (Worcester, MA) and were previously validated [36]. AT1aR-Cre-Zsgreen knock-in mice were bred with stop-flox-tdTomato mice (Jackson Laboratory, Bar Harbor, ME, stock #007914) to generate AT1aR-tdTomato mice for mapping Cre-recombinase expression throughout the brain regions of interest (ROIs). (2) AT2R-eGFP BAC reporter mice were generated as detailed previously [16]. (3) AT1aR-tdTomato/AT2R-eGFP dual-reporter mice were produced by crossing AT1aR-tdTomato reporter mice and AT2R-eGFP BAC reporter mice. In these mouse strains, the tdTomato (AT1aR) signal reflects cells that expressed AT1aRs at any time in their developmental history. In contrast, the eGFP (AT2R) signal reflects the current expression of AT2R. Further, while these strains allow for the identification of cells that contain AT1aR and AT2R, they do not demonstrate where the receptors are located within the cells.

Rats

Age-matched 12- and 16-week-old male Sprague-Dawley (SD), Wistar Kyoto (WKY), and spontaneously hypertensive rats (SHR) were purchased from Charles River Farms (Wilmington, MA).

DOCA-salt hypertension

In some studies, mice were rendered hypertensive via the administration of DOCA and subsequent ad libitum access to an isotonic saline drink (0.15 M NaCl) in addition to continued access to standard drinking water [37, 38]. In these studies, DOCA pellets (50 mg, Innovative Research of America, Sarasota, FL) were implanted subcutaneously in the interscapular region. Immediately after pellet implantation, the mice were provided free access to an isotonic saline drink for the 3-week duration of the study. Controls underwent sham pellet implantation surgery.

Blood pressure recordings

To confirm that DOCA-salt administration elevated blood pressure in mice, we measured blood pressure using the

volume–pressure recording tail cuff method (Kent Scientific, Torrington, CT). Briefly, the mice were restrained and placed on a warming platform. An occlusion cuff was placed close to the base of the tail, and a VPR cuff was then placed next to the occlusion cuff. Both the occlusion and VPR cuffs were connected to a CODA controller (Kent Scientific, Torrington, CT) that was connected to a computer. The blood pressure signal from the tail cuff was recorded and analyzed using a CODA Noninvasive Blood Pressure System. Blood pressure in each mouse was recorded for seven cycles to minimize recording error.

Tissue collection and sectioning

Mice or rats were anesthetized with pentobarbital and perfused transcardially with 0.15 M NaCl followed by 4% paraformaldehyde. Brains were postfixed for 4 h, after which they were stored in 30% sucrose until sectioning using a CM3050S cryostat (Leica, Buffalo Grove, Illinois). For in situ hybridization, perfused brains were sectioned at 20 µm into six serial sections and immediately mounted onto SuperFrost Plus Gold Microscope Slides. After air-drying at room temperature for 20–30 min, the slides were stored at −80 °C. Tissue collection and sectioning were performed in RNase-free conditions. For immunohistochemistry (IHC) studies, brains were sectioned at 30 µm into four serial sections and stored in a cryoprotective solution at −20 °C.

Immunohistochemistry

All primary antibodies had been characterized by their manufacturer and in previously published studies (Supplementary Table 1) [39–48]. Secondary antibodies were purchased from Jackson ImmunoResearch, raised in a donkey and used at a 1:500 dilution. All IHC protocols used were previously described by us [16, 35, 49] and performed in at least four separate mice/rats. Importantly, for studies conducted in AT1aR-tdTomato/AT2R-eGFP dual-reporter mice, GFP IHC was performed using a Cy5-labeled secondary antibody. This protocol did not produce significant labeling in mice that expressed only AT1aR-tdTomato but not AT2R-eGFP.

RNAscope in situ hybridization

RNAscope in situ hybridization for AT1aR mRNA was performed as described [16]. The probes were designed using the proprietary Advanced Cell Diagnostics (Newark, CA) RNAscope Probe Design pipeline and comprised 20 short double-Z oligonucleotide probe pairs that were specific to the genes of interest (i.e., AT1aR, UBC [positive control], and DapB [negative control]). Details concerning the probes used for RNAscope in situ hybridization can be found in Supplementary Table 2. The color label was assigned to FAR RED (excitation 647 nm; emission 690 ± 10 nm). Importantly, using this technique, each punctate dot represents a single-mRNA molecule.

Image capture and processing

Images were captured and processed using a Zeiss AxioImager fluorescent apotome microscope and AxioVision 4.8.2 software, respectively. To generate images of the entire coronal sections depicted in Supplementary Fig. 1 and Fig. 1, images magnified ×2.5 were captured across the various points of each section. Subsequently, ImageJ was used to generate stitched mosaic images comprising coronal sections taken through specific levels of the forebrain or hindbrain. These mosaics were used for the analysis, reported in Supplementary Table 3.

For the IHC studies shown in Figs. 2, 3, and 5, images were captured at ×5 to ×10, and z-stacks were captured at ×20 throughout the ROIs using neuroanatomical landmarks found in a mouse brain atlas [50]. In these cases, the exposure time was adjusted using the best fit feature in AxioVision to provide optimal visualization. For dual IHC/RNAscope ISH experiments shown in Fig. 4, z-stacks of the proteins and transcripts of interest were captured at ×20 magnification throughout the ROIs. In all cases, z-steps were set at 0.5 µm, with an average of 20 optical sections per image, and these z-stacks were used to generate the projection images displayed in the photomicrographs. For each dual IHC/RNAscope ISH experiment, sections hybridized with the positive control probes were used to determine the exposure time and image processing required for optimal visualization of the RNA signal. As described, these same parameters were then used to visualize mRNA transcripts of interest and to assess background fluorescence in sections hybridized with negative control probe (DapB) [16]. Importantly, using these exposure times and image processing parameters, there was negligible fluorescence in sections hybridized with the negative control probe.

All final figures were then prepared using Adobe Photoshop 7.0, in which brightness and contrast were adjusted to provide optimal visualization.

Analysis of AT1aR- and AT2R-expressing neurons

Mosaics of coronal sections through four separate mouse brains were analyzed to determine the number of tdTomato-positive cell bodies and/or the presence of tdTomato fibers or terminals within brain regions important for cardiovascular function, fluid balance, and metabolism. The number of sections analyzed was dependent on the rostrocaudal length of the particular ROI analyzed. For example, only two sections through the OVLT were analyzed for each mouse, whereas

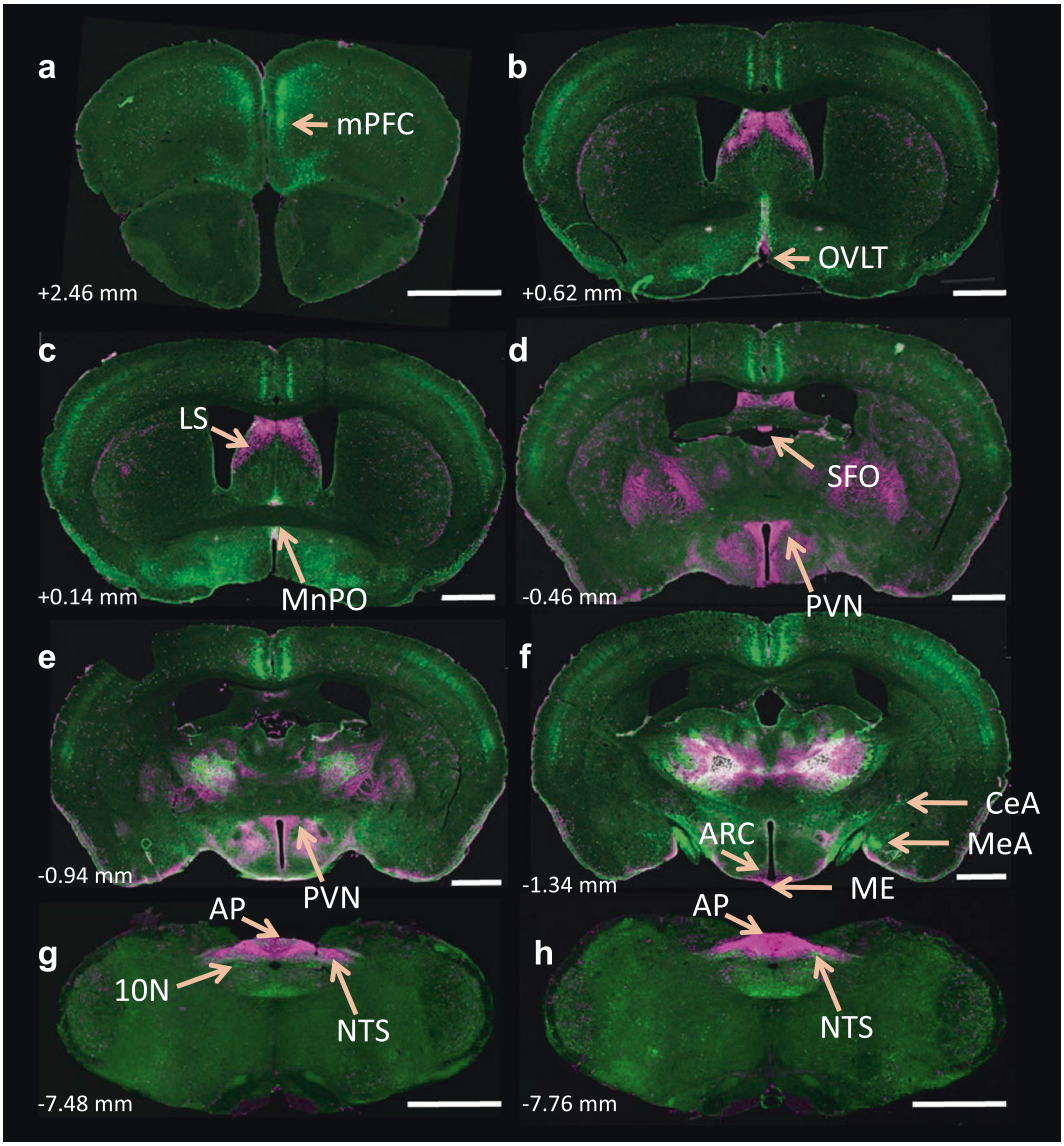

Fig. 1 Localization of tdTomato and eGFP fluorescence throughout the brain of a dual AT1aR-tdTomato/AT2R-eGFP reporter mouse. **a**–**h** Low-magnification coronal sections through selected brain regions of a male dual AT1aR-tdTomato/AT2R-eGFP reporter mouse. AT1aR-tdTomato fluorescence is indicated in magenta; AT2R-eGFP fluorescence is indicated in green. The number in the lower left of each image indicates the approximate distance rostral/caudal from bregma in accordance with the mouse brain atlas [50]. mPFC medial prefrontal cortex, MnPO median preoptic nucleus, LS lateral septum, AH anterior hypothalamus, PVN paraventricular nucleus of the hypothalamus, MeA medial amygdala, CeA central amygdala, NA nucleus ambiguus, NTS nucleus of the solitary tract, 10N = dorsal motor nucleus of the vagus, AP area postrema. Scale bars = 1 mm. These images are representative of eight mice

~15 sections throughout the NTS were analyzed for each mouse. Criteria used to score and count AT1aR-positive cell bodies were as follows: 0 = no tdTomato-positive cells within the ROI, 1 = 1–25% of the area occupied by tdTomato-positive cell bodies, 2 = 26–50% of the area occupied by tdTomato-positive cell bodies, 3 = 51–75% of the area occupied by tdTomato-positive cell bodies, and 4 = 76–100% of the area occupied by tdTomato-positive cell bodies. All sections were analyzed by two separate investigators, following which the mean score for each brain region was calculated and rounded to the nearest whole number. Brain regions that received a score between 0 and 0.5 are listed as <1. The presence of fibers or terminals was assessed in the same sections, and sections were scored as + (indicating scattered fibers/terminals present within the ROI), ++ (indicating dense fibers/terminals present within the ROI) or − (indicating that no fibers/terminals were observed within the ROI).

Analysis of AT1aR-tdTomato and AT2R-eGFP colocalization was performed by two independent investigators on 10× z-stacks throughout the ROIs of four male and four female AT1aR-tdTomato/AT2R-eGFP dual-reporter

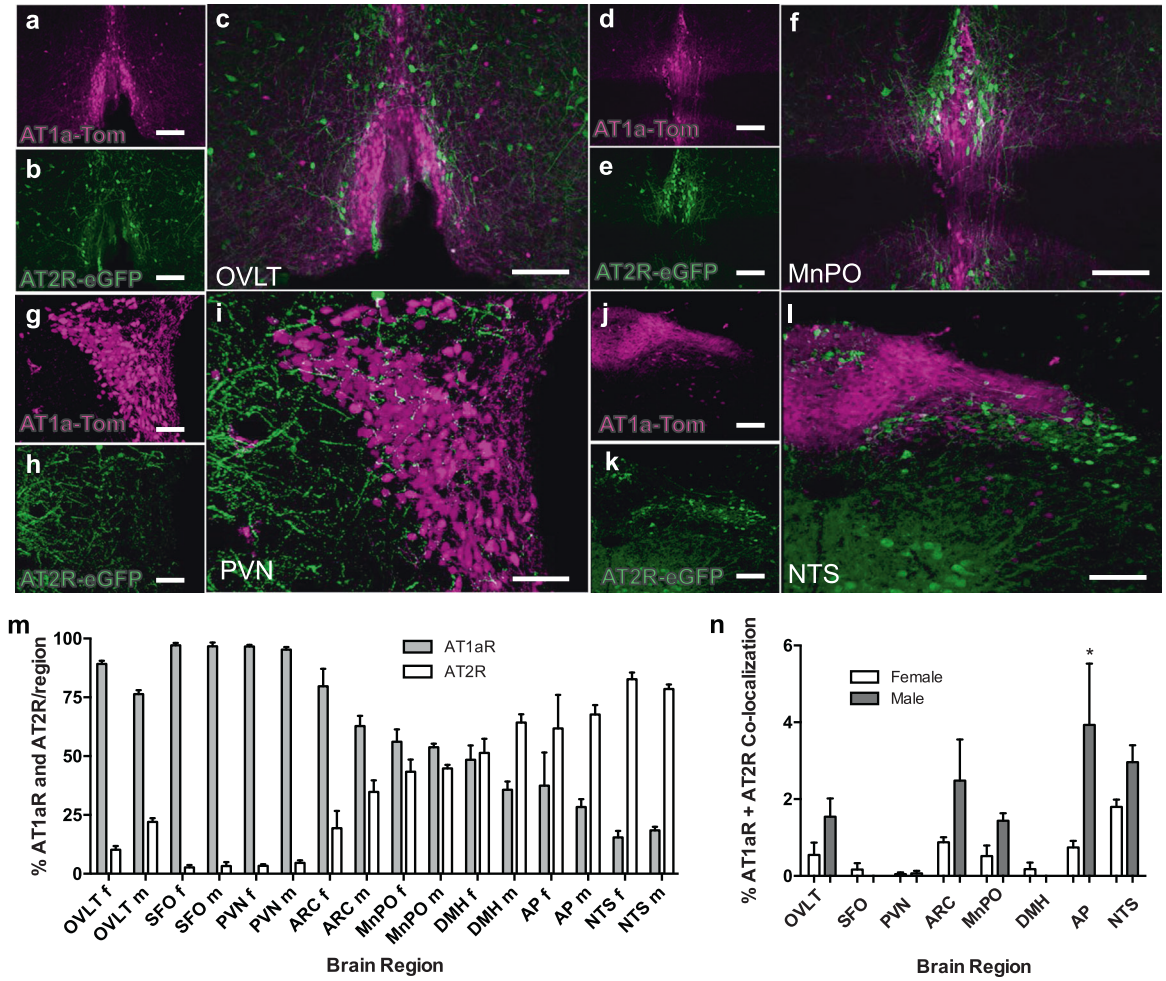

Fig. 2 Relative localization of tdTomato and eGFP fluorescence within the OVLT, MnPO, PVN, and NTS of a dual AT1aR-tdTomato/AT2R-eGFP reporter mouse. High-magnification images of the OVLT (**a**, **b**), MnPO (**d**, **e**), PVN (**g**, **h**), and NTS (**j**, **k**) of a male dual AT1aR-tdTomato/AT2R-eGFP reporter mouse showing AT1aR-tdTomato (magenta) and AT2R-eGFP (green). The respective merged images are shown in **c** (OVLT), **f** (MnPO), **i** (PVN), and **l** (NTS). Scale bars = 100 µm (**a**, **b**, **d**, **e**, **g**, **h**, **j**, and **k**) and 50 µm (**c**, **f**, **i**, and **l**). These images are representative of eight mice. Bar graphs in **m** and **n** show the relative levels of AT1aR- and AT2R-positive cells within the selected brain regions of female and male AT1aR-tdTomato/AT2R-eGFP reporter mice. **m** The percentages of cells expressing AT1aR and AT2R within the regions indicated are plotted as the means ± SEMs for both female [f] and male [m] mice. OVLT organum vasculosum of the lamina terminalis, SFO subfornical organ, PVN paraventricular nucleus, ARC arcuate nucleus, MnPO median preoptic nucleus, DMH dorsomedial hypothalamus, AP area postrema, NTS nucleus of the solitary tract. Data are from four female and four male AT1aR-tdTomato/AT2R-eGFP reporter mice. **n** The percentage of cells within the selected regions showing the colocalization of AT1aR and AT2R are plotted as the means ± SEMs for both female and male mice. $^*P < 0.05$ vs. female AP

mice. To determine the percent expression of AT1aR vs. AT2R and their colocalization within these areas, the total number of AT2R-eGFP-positive, AT1aR-tdTomato-positive, and double-labeled neurons were assessed. To determine colocalization of AT1aR-tdTomato and microglial (Iba-1), astrocyte (GFAP), and neuronal (HuC/D) markers within the PVN of normotensive ($n = 4$) vs. DOCA-salt hypertensive ($n = 4$) mice, sections throughout the area were evaluated by the two independent investigators. A similar procedure was used to evaluate the colocalization of AT2R-eGFP and microglial (Iba-1), astrocyte (GFAP), and neuronal (HuC/D) markers within the NTS ($n = 4$/group).

Analysis of astrocyte area fraction

The astrocyte area fraction within the rat PVN indicated by the level of GFAP immunostaining was quantified by ImageJ (NIH)-mediated analysis of fluorescence micrographs obtained from the anterior, medial, and posterior PVN and identification using neuroanatomical landmarks described by Paxinos and Watson [51]. PVN ROIs were then converted into grayscale and binary formats, and the thresholds for black and white balance were adjusted to the same levels for each ROI. At each PVN level, counts from both sides of the PVN were collected and averaged. Quantified results were plotted as the percentage of GFAP-

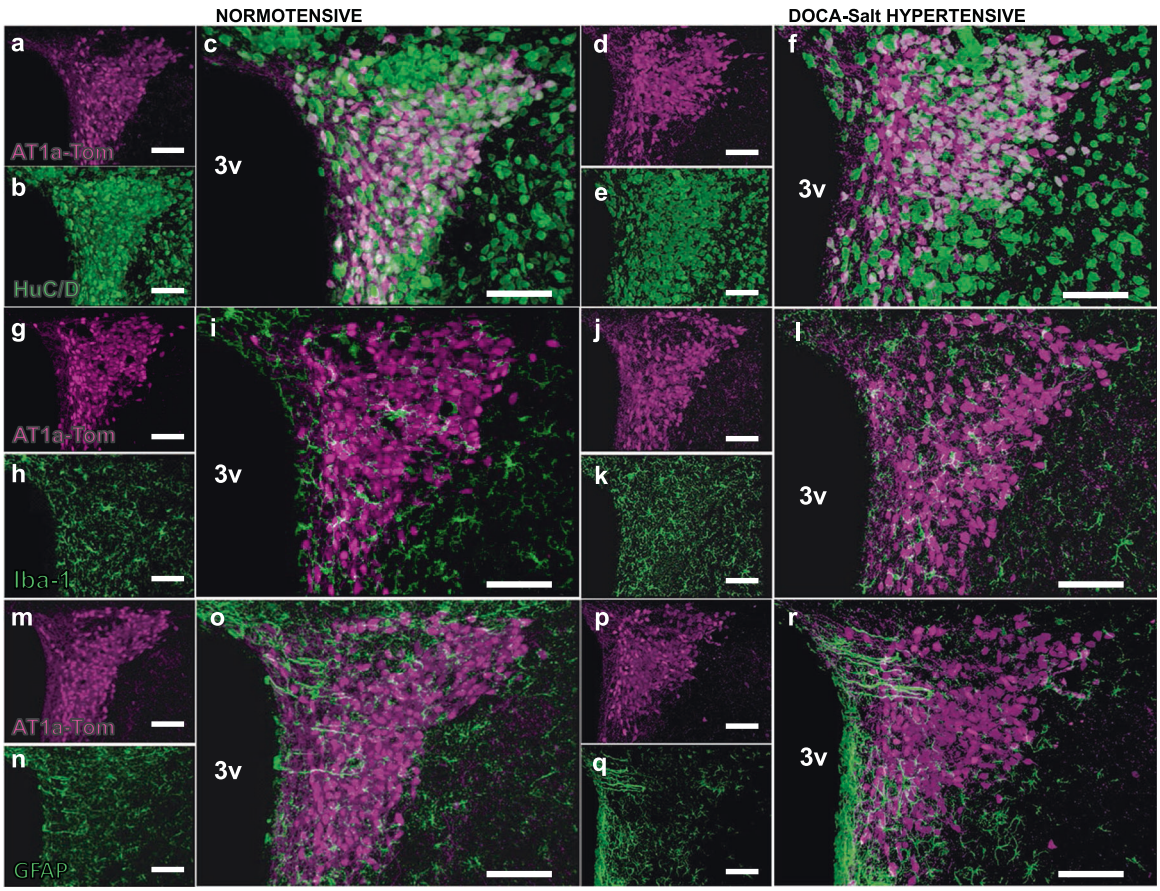

Fig. 3 Cellular localization of AT1aR-positive cells within the PVN of normotensive and DOCA-salt hypertensive mice. Projection images from the PVNs of male normotensive and DOCA-salt hypertensive mice showing the location of AT1aR-tdTomato fluorescence in relation to neurons, microglia, and astrocytes. The location of tdTomato fluorescence (magenta) is illustrated in **a**, **g**, and **m** (control normotensive mice) and **d**, **j**, and **p** (DOCA-salt hypertensive mice). **b** and **e** demonstrate HuC/D (neuron-specific marker; green) immunostaining of the same sections shown in **a** and **d**, respectively. The merged images (**c**, **f**) illustrate that tdTomato fluorescence is entirely associated with HuC/D staining. **h** and **k** demonstrate Iba-1 (microglial marker; green) immunostaining of the same sections shown in **g** and **j**, respectively, while **n** and **q** demonstrate GFAP (astrocyte marker; green) immunostaining of the same sections shown in **m** and **p**, respectively. The merged images (**i** and **l** for Iba-1; **o** and **r** for GFAP) indicate that tdTomato fluorescence is not associated with microglia or astrocytes. 3 V = 3rd cerebroventricle. These images are representative of four mice/group. Scale bar = 100 μm

positive cells in each ROI. The astrocyte area fraction in the anterior portion of the PVN exhibited no change under any of the tested conditions, so the data presented in the "Results" section of this manuscript are from the medial (−1.44 mm) and posterior (−2.16 mm) levels of the PVN [coordinates from the bregma].

Results

AT1aR-tdTomato reporter mice

We developed an AT1aR-tdTomato reporter mouse strain that was used in the two following ways in this manuscript: (1) to generate a novel AT1aR-tdTomato/AT2R-eGFP dual-reporter mouse line by crossing AT1aR-tdTomato reporter mice with our existing AT2R-eGFP BAC reporter mice and (2) to study the cellular localization of AT1aR in neurons vs. glia during hypertension. Before these experiments, it was important to perform certain experiments to characterize the AT1aR-tdTomato reporter mice. First, as noted in the "Materials and methods" section, the tdTomato (AT1aR) fluorescence signal not only indicates cells that currently express AT1aR but also reflects cells that may have expressed AT1aR at an earlier developmental stage. The extent to which tdTomato fluorescence is indicative of *current* AT1aR expression was assessed in a previous study via the in situ hybridization of AT1aR mRNA in tissue sections collected from AT1aR tdTomato reporter mice [36], which demonstrated that ~97% of tdTomato-positive neurons within the PVN contained AT1aR mRNA [36]. Second, it was important to demonstrate that the pattern of AT1aR expression within the AT1aR-tdTomato reporter mouse brain indicated by tdTomato fluorescence was

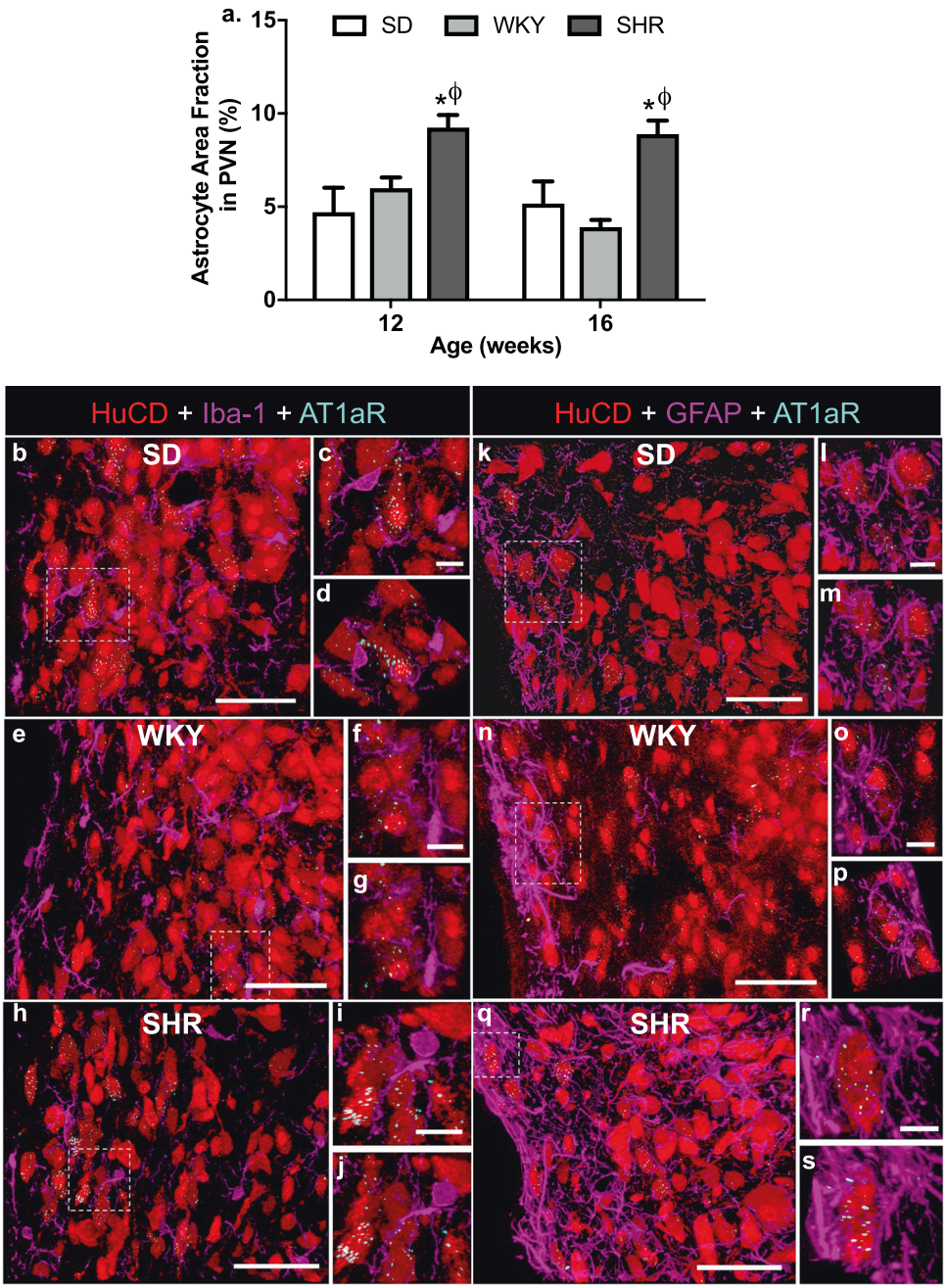

Fig. 4 Cellular localization of AT1aR mRNA in the PVNs of normotensive rats and SHR. **a** Naive male SD, WKY, and SHR were prepared for GFAP immunostaining of the PVN as detailed in the "Methods" section. The bar graph shows the quantification of GFAP immunoreactivity within the PVNs of 12- and 16-week-old SD, WKY, and SHR rats using ImageJ. Data are presented as a summation of the astrocyte area fraction in the *medial and posterior* PVN (means ± SEMs) for each set of rats and are from four SHR, three WKY, and four SD rats at 12 and 16 weeks of age. $^{*}p < 0.05$ SHR vs. SD; $^{\Phi}p < 0.05$ SHR vs. WKY. **b**–**s** Representative fluorescence images showing the localization of Iba-1 (left, **b**–**j**) and GFAP (right, **k**–**s**) immunoreactivity (*both magenta*) in the PVNs of SD, WKY, and SHR rats. Immunoreactivity for the neuronal marker HuCD is shown in *red*, and AT1aR mRNA is indicated by *cyan* dots. The higher-power images (**c**, **d**; **f**, **g**; **I**, **j**; **l**, **m**; **o**, **p**; **r**, **s**) are from the areas indicated by the hashed lines in the corresponding lower-power images. Each higher-power image was taken at two different angles to determine the discrete cellular localization of AT1aR mRNA. Sections are from the medial PVN ~−1.8 mm relative to the bregma [51] and are representative of three (WKY) or four (SD; SHR) rats. Sections taken from more rostral or caudal parts of the PVN exhibited a similar cellular distribution of AT1aR. Scale bars for lower-power images = 50 μm; scale bars for higher-power insets = 10 μm

generally consistent with that observed in previous studies that utilized receptor autoradiography, radioactive in situ hybridization, and transgenic reporter mice to assess AT1aR localization in rodent brains [10–15]. This is illustrated in

Supplementary Fig. 1, which contains representative fluorescence micrographs of coronal brain sections through the subfornical organ (SFO), OVLT, PVN, median preoptic nucleus (MnPO), and area postrema (AP) of a male mouse. These illustrations demonstrate that within the AT1aR-tdTomato reporter mouse brain, tdTomato fluorescence is present in areas important for cardiovascular function, fluid balance and metabolism. In addition, Supplementary Table 3 presents a survey of AT1aR-tdTomato-positive cells and fibers throughout these specific sections, with an emphasis on brain nuclei important for cardiovascular function, fluid balance and metabolism. This distribution is largely consistent with the known distribution of AT1aR in the brain demonstrated in previous studies [10–15]. Notably, although the AT1aR-Cre knock-in mouse strain used to generate AT1aR-tdTomato reporter mice was intended to also express zsGreen in AT1aR-containing cells, zsGreen fluorescence was not observed in the brains of these mice, nor did IHC using primary antibodies that detect GFP amplify any type of zsGreen signal. Based on the collective results of these studies, we believed that the AT1aR tdTomato reporter mouse strain was an appropriate model to crossbreed with our AT2R-eGFP BAC reporter mouse strain to produce a novel AT1aR-tdTomato/AT2R-eGFP dual reporter mouse strain and for use in investigating the neuronal/glial localization of AT1aR in hypertension.

AT1aR and AT2R are localized primarily to separate populations of neurons

Several lines of evidence suggest that AT1R and AT2R activation counteract one another via opposing intracellular signaling cascades [52]; however, direct evidence showing the localization of AT1R and AT2R to the *same cells* within the brain is limited. For the present studies, we generated a dual AT1aR-tdTomato/AT2R-eGFP mouse line by crossbreeding AT1aR-tdTomato and AT2R-eGFP BAC reporter mice and performed an analysis of the colocalization of the two receptor subtypes within brain areas important in regulating the cardiovascular system, fluid balance and metabolism. Figure 1 depicts representative low-power fluorescence micrographs from the coronal brain sections of a male dual reporter mouse and provides a stark visualization of the mostly distinct localization of AT1R (magenta)- and AT2R (green)-positive cells in the mouse brain. This distinct localization is particularly apparent in the brain areas of specific interest to the current study, as shown in Fig. 2, which includes representative fluorescence images at higher magnification showing AT1aR-tdTomato/AT2R-eGFP fluorescence in the OVLT (a–c), MnPO (d–f), PVN (g–i), and NTS (j–l). Analyses of the relative levels of AT1aR- and AT2R-positive cells within brain sections obtained from male and female mice are shown in Fig. 2m; these analysis revealed the following: (1) The OVLT, SFO, PVN, and arcuate nucleus (ARC) contained greater levels of AT1aR-expressing vs. AT2R-expressing cells, while the opposite was true for the NTS and AP. (2) A number of AT1aR- and AT2R-positive cells in the MnPO were roughly equal. (3) In most cases, there were no sex-related differences in the absolute numbers of AT1aR- and AT2R-positive cells from region to region. An exception was the dorsomedial nucleus of the hypothalamus (DMH); the DMHs of females contained almost equal number of AT2R-negative and AT2R-positive cells, but those of males contained more AT2R-positive cells. Analyses of the colocalization of the two receptor subtypes in individual cells revealed that only a minority of the cells within these ROIs contained both AT1aR and AT2R (Fig. 2n). In fact, within the SFO, PVN, and DMH, AT1aR and AT2R colocalization was observed in <0.2% of the total population when both subtypes were present. In the other regions examined, the colocalization of these receptor subtypes was scarcely higher and ranged from 0.5 to 3.9%; interestingly, receptor colocalization was more common in males in all cases, and this difference was significant in the AP (Fig. 2n). However, the overall implication from these studies is that in these brain regions, AT1aR and AT2R are localized primarily to separate neurons.

Cellular localization of AT1aR in the PVN under baseline conditions and during hypertension

Analysis of both normotensive dual AT1aR-tdTomato/AT2R-eGFP reporter mice and normotensive AT1aR-tdTomato reporter mice revealed that AT1aR-positive cells within the brain were mostly neuronal-like. Because the prohypertensive activity of AT1R involves the stimulation of proinflammatory mechanisms in the brain [53], we investigated the cellular distribution of AT1aR during DOCA-salt-induced hypertension, an experimental model of neurogenic hypertension. Specifically, we utilized AT1aR-TdTomato reporter mice to determine whether AT1aR expression was increased in the resident inflammatory cells of the CNS, microglia, and astrocytes [36], during hypertension. We focused on the PVN because it is a major center for sympathetic and neuroendocrine control [54], because the formation of lesions in the PVN was shown to prevent the development of hypertension in DOCA-salt treated rats and in SHR [55, 56], and because previous studies demonstrated the increased expression of AT1aR and AT1R mRNA in this area in hypertensive animals [18, 57]. Sham or DOCA pellets were implanted in AT1aR-tdTomato reporter mice, and the mice were given ad libitum access to an isotonic saline drink in addition to their normal drinking water. After 3 weeks, systolic blood pressure in the DOCA-treated mice (112.0 ± 4.57 mmHg; $n = 4$) was significantly higher than that in the controls (87.99 ± 2.88

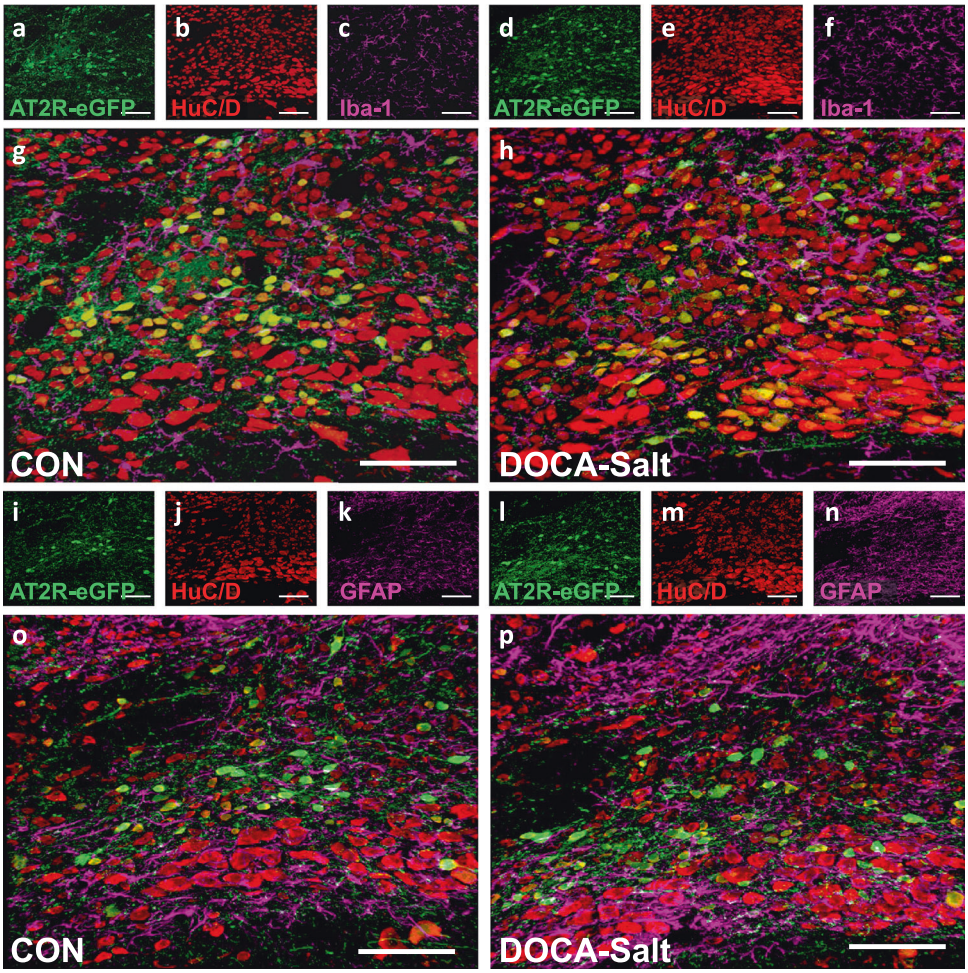

Fig. 5 Cellular localization of AT2R-positive cells within the intNTSs of normotensive and DOCA-salt hypertensive mice. Projection images through the intNTSs of male control normotensive and DOCA-salt hypertensive mice showing the location of AT2R-eGFP fluorescence (green) relative to neurons, microglia, and astrocytes. **a–c**, **g** CON or (**d–f**, **h**) DOCA-salt AT2R-eGFP mice depicting eGFP (**a**, **d**), HuC/D (**b**, **e**), and Iba-1 (**c**, **f**) immunoreactivity and the corresponding merged images (**g**, **h**). **i–k**, **o** CON or (**l–n**, **p**) DOCA-salt AT2R-eGFP mice depicting eGFP (**i**, **l**), HuC/D (**j**, **m**), and GFAP (**k**, **n**) immunoreactivity and the corresponding merged images (**o**, **p**). These images are representative of eight mice/group. Scale bars correspond to 100 μm

mmHg; $n = 4$; $t(6) = 4.45$; $p = 0.002$). Following blood pressure measurements, the mice were euthanized for immunohistochemical studies. Figure 3 depicts representative coronal sections through the PVNs of DOCA-salt-treated or control AT1aR reporter mice that were immunohistochemically labeled for microglial, astrocyte or neuronal markers. As expected, under both baseline and hypertensive conditions, there was a significant overlap between AT1aR-tdTomato fluorescence (magenta) and the neuronal marker HuC/D (green; Fig. 3a–f). The control normotensive mice exhibited no overlap between AT1aR-tdTomato fluorescence and either the microglial (Iba-1) or astrocyte (GFAP) markers throughout the PVN (Fig. 3g–i, m–o). This finding was largely expected given previous publications that indicated that AT1R is almost exclusively localized to neurons in the brain in vivo [15, 58]. Interestingly, in DOCA-salt-treated hypertensive mice, there was also no overlap between AT1aR-tdTomato fluorescence and microglial (Iba-1) or astrocyte (GFAP) markers in the PVN (Fig. 3j–l, p–r). Similar results were obtained when the MnPO, SFO, AP, and NTS were probed to assess the colocalization of tdTomato with HuC/D, GFAP, or Iba-1 (data not shown).

SHR are another experimental model of neurogenic hypertension, and previous studies indicated that SHR with established hypertension (12–21 weeks old) exhibit increased numbers and activation of microglia within the PVN [59]. Our current immunostaining experiments and quantification of the GFAP-positive astrocyte area fraction within the PVN (medial to posterior regions) of 12- and 16-week-old SHR indicated significantly more astrocytes in SHR compared with normotensive SD and WKY rats (Fig. 4a). Despite the increased numbers and activation of astrocytes and microglia in the PVNs of SHR with established hypertension, RNAscope analyses of AT1aR mRNA provided no evidence for the presence of this angiotensin receptor subtype on these glial cells within the SHR PVN. This is illustrated in Fig. 5b–s, which shows representative coronal sections through the medial PVN of a 12-week-old SHR and those of age-matched WKY and SD rats. Fig 4b, e, and h shows low-power images from the PVNs of SD, WKY rats, and SHR, respectively, indicating that AT1aR mRNA (*cyan* dots) is associated with neurons (*red*, HuCD-positive) but not microglia (*magenta*, Iba-1-positive). This cellular distribution was confirmed by high-power

micrographs that were taken in two different planes (Fig. 4c, d [SD]; Fig. 4f, g [WKY]; Fig. 4i, j [SHR]). Similarly, Fig. 4k–m, n–p, and q–s shows that AT1aR mRNA is associated with neurons and not astrocytes (magenta, GFAP-positive) in the PVNs of SD, WKY, and SHR, respectively.

Cellular localization of AT2R in the NTS under baseline conditions and during hypertension

Preliminary observations from normotensive AT1aR-tdTomato/AT2R-eGFP dual-reporter mice suggested that AT2R-positive cells within the brain are mostly neuronal-like, consistent with our previous observation from AT2R-eGFP BAC reporter mice [16]. However, some antihypertensive activities mediated by brain AT2R involve the induction of anti-inflammatory mechanisms [18]. Thus, using AT2R-eGFP reporter mice, we examined the expression of AT2R on microglia and astrocytes during DOCA-salt-induced hypertension. For these experiments, we focused on the intermediate NTS (intNTS) because it contains one of the largest populations of AT2R in the brain (Fig. 2) [60], and studies have indicated that activation of AT2R in the NTS modulates blood pressure and baroreflex function [23, 27–29]. The fluorescence micrographs shown in Fig. 5a–c, g, i–k and, o indicate that under control normotensive conditions, AT2R-eGFP in the intNTS is colocalized entirely with neurons (HuC/D-positive) and that no colocalization of AT2R-eGFP with either Iba-1-positive microglia or GFAP-positive astrocytes was observed, as expected. The cellular localization of AT2R was unchanged during DOCA-salt-induced hypertension, i.e., AT2R-eGFP was associated with neurons and not microglia or astrocytes (Fig. 5d–f, h, l–n, p).

Discussion

The major novel findings of this study are the following: (1) We developed an AT1aR-tdTomato reporter mouse strain that was crossed with our existing AT2R-eGFP BAC reporter mouse strain to yield a novel AT1aR/AT2R dual-reporter mouse strain. (2) This AT1aR-tdTomato/AT2R-eGFP dual-reporter mouse strain was used to reveal the relative cellular localization of AT1aR/AT2R in the adult brain; while they were localized primarily to different populations of neurons, in a few cases, neurons expressed both. (3) In AT1aR-tdTomato reporter mice made hypertensive via chronic DOCA-salt treatment, there was no shift in expression of AT1aR in the PVN from neurons to microglia or astrocytes. This finding was confirmed in SHR, another model of neurogenic hypertension, in which there was also no difference in the neuronal vs. glial distributions of AT1aR in the PVN compared with WKY and SD normotensive rats. (4) In AT2R-eGFP BAC reporter mice made hypertensive via chronic DOCA-salt treatment, there was no shift in expression of AT2R in the intNTS from neurons to microglia or astrocytes.

In the transgenic AT1aR-tdTomato reporter mouse strain used in the present study, the distribution of tdTomato fluorescence was predominantly consistent with the previous results of in situ hybridization, receptor autoradiography, and AT1aR reporter mouse studies with respect to regional localization [10–15, 61]. For example, and as expected, key cardiovascular, fluid homeostasis, and neuroendocrine control centers in the brain, the SFO, OVLT, PVN, MnPO, NTS, and AP, were rich in AT1aR-positive cells and fibers, consistent with previous studies. The location of AT1aR in these areas, as evidenced by findings from the AT1aR reporter mice, was consistent with the following well-described AT1R-mediated actions of Ang-II at these brain sites: water and salt intake in the SFO and OVLT [62–65]; sympathetic outflow, blood pressure regulation, energy balance, and corticotropin-releasing hormone (CRH) secretion in the PVN [60, 66–68]; renal and cardiovascular regulation and water intake in the MnPO [69, 70]; baroreflex and blood pressure control in the NTS [71, 72]; and sympathetic outflow and blood pressure control in the AP [73, 74]. Therefore, the present studies corroborate the validity of the AT1aR-Cre mouse line as well as the utility of the AT1aR-tdTomato mouse line to detect AT1aR localization. Based upon this, our AT1aR-tdTomato mouse line could be used to provide a detailed characterization of the *phenotype* of AT1aR-localized cells throughout the brain. Knowledge of the identity of AT1aR-containing cells could then be used to assess the functions of these receptors. For example, in a recent study using this mouse strain, we demonstrated that with regard to neurons that originate in the PVN, AT1aRs were located on neurons that project to the median eminence and secrete CRH and thyrotropin-releasing hormone [36], consistent with the ideas put forth by Lenkei et al. [58] and Oldfield et al. [75] using traditional IHC and in situ hybridization approaches. Furthermore, optogenetic activation of these AT1aR-containing neurons significantly elevated the levels of plasma adrenocorticotrophic hormone, corticosterone, thyroid-stimulating hormone and thyroxine [36]. In the same study, we demonstrated that preautonomic neurons that project to the RVLM do not contain AT1aR [36], suggesting that increased blood pressure resulting from the stimulation of AT1aR in the PVN is not the direct effect of Ang-II on sympathetic pathways. With the anatomical knowledge gained from the AT1aR reporter mouse strain, our future studies will target the functionality of AT1aR-containing neuron populations in areas beyond the PVN, such as the MnPO.

However, the use of the AT1aR-tdTomato mouse strain to perform a detailed analysis of the phenotype of AT1aR-containing neurons was not a goal of the present study. Rather, we utilized this mouse strain to help produce an AT1aR/AT2R dual-reporter mouse strain and to help to determine the cellular distribution of brain AT1aR during hypertension. With regard to the former, the AT1aR-tdTomato/AT2R-eGFP dual-reporter mouse strain has allowed for the visualization and comparison of the *discrete* cellular localization of AT1aR and AT2R in the brain. Previous receptor autoradiography techniques in rats and humans [11, 12, 61, 76–78] illustrated the regional/area distribution of AT2R in the brain, and the early conclusions of these studies were that AT1R and AT2R exhibit mostly exclusive localization, with the former present in areas important in cardiovascular and fluid balance regulation, and the latter present in brain areas that control sensory and cortical functions. However, in situ hybridization studies revealed that AT2R is present in areas important in cardiovascular regulation, such as the NTS [10]. Further, our recent study using adult AT2R-eGFP reporter mice has provided a more discrete view of AT2R localization in the brain, including the presence of AT2R within or adjacent to areas important for cardiovascular regulation and fluid balance, such as the NTS, AP, MnPO, OVLT, and SFO [35]. The AT1aR-tdTomato/AT2R-eGFP dual reporter mouse strain developed here and used in the present study has confirmed this localization. Any apparent differences in the locations of AT1aR and AT2R in the brains of rats and humans gained from receptor autoradiography compared with their locations in the reporter mice used in the present study could be due to a number of the following reasons. (1) Species differences could account for these discrepancies. (2) As mentioned earlier, tdTomato fluorescence in the AT1aR reporter mice, and indeed eGFP fluorescence in AT2R-eGFP BAC reporter mice, do not reveal where the receptors reside *within* cells. So, for example, the presence of eGFP fluorescence in the cell bodies of neurons close to the OVLT may not necessarily mean that AT2R are located on these cell bodies; they may be located where the terminals of those neurons reside, potentially at a distant site. This could explain possible discrepancies with autoradiographic studies, which should reveal the general area where the receptors are located. (3) Because the reporter mouse model enables the discrete detection of these receptors to individual cells, cells in the mice with low expression of AT1aR or AT2R can now be visualized, whereas this may not have been possible with the receptor autoradiography technique used in rats and humans.

Our current studies using the AT1aR-tdTomato/AT2R-eGFP dual-reporter mouse strain have revealed that in certain brain areas, the number of AT2R-positive neurons exceeds, or is at least equal to, the number of AT1R-positive neurons (Fig. 2m). Our studies have also demonstrated that AT1R and AT2R are largely (>95%) expressed on separate populations of neurons and that there are no sex-related differences in the expression of these receptors (Fig. 2m). Interestingly; however, in situations in which these receptors are colocalized on the same neuron (in the OVLT, ARC, MnPO, AP, and NTS; ~1–4% overlap), there is a stronger tendency for this colocalization to be in males vs. females (Fig. 2n). Based on the largely exclusive expression of AT1R and AT2R to separate populations of neurons in brain regions that control cardiovascular function, fluid homeostasis and metabolism, one might speculate that the functional effects of these receptors are mediated via separate mechanisms; for example, the opposite effects on blood pressure and baroreflex function may be mediated by different neuronal circuitry, as we proposed previously [19]. Despite this, and even though the proportion of cells exhibiting the colocalization of AT1R and AT2R never exceeded 4%, we cannot exclude at this point the possibility that intracellular interactions between these receptors have a role in controlling cardiovascular function, fluid homeostasis, and metabolism.

One thing that is apparent from the present study and our previous studies using AT1aR-tdTomato reporter, AT2R-eGFP reporter, and the dual-reporter mice is that in normal, adult animals, AT1R and AT2R are localized to neurons, and not astrocytes or microglia, in the areas studied (the PVN, MnPO, NTS, AP, and OVLT). This is in concert with previous publications indicating that within the normal brain in vivo, AT1R and AT2R are localized almost exclusively to neurons, rather than astrocytes or microglia [10, 15, 58, 79, 80]. Previous studies demonstrated the increased expression of AT1R in the PVNs of hypertensive animals [18, 57]. Thus, we wanted to determine whether AT1Rs are also expressed in glia at this site during hypertension. Our results indicated that under conditions of neurogenic hypertension, in AT1aR-tdTomato reporter mice made hypertensive by the administration of DOCA-salt (Fig. 3) and SHR (Fig. 4), the AT1aR-tdTomato fluorescence signal was localized to only PVN neurons and was not found on glia. Interestingly, in other studies, we observed increased levels of AT2R mRNA within the same population of neurons in the intNTS of DOCA-salt hypertensive mice (de Kloet et al. unpublished data). Consistent with this, it is clear from the data in Fig. 5 in the current study that following DOCA-salt-induced hypertension, AT2R-eGFP fluorescence remained localized to neurons and was not associated with astrocytes or microglia. It will be interesting to determine whether a similar pattern of cellular AT1aR and AT2R location is evident in other forms of hypertension, such as obesity-induced hypertension or renovascular hypertension.

Concerning the PVN and neurogenic hypertension, the possible localization of AT1aRs exclusively to neurons at this site has a number of implications for the mechanisms underlying chronic sympathoexcitation and the neuroinflammatory processes that occur during sustained high blood pressure [30, 81, 82]. For example, this suggests that the microgliosis that occurs in the PVN in hypertension involving Ang II/AT1aR is not due to the *direct* actions of Ang II at AT1R on microglia. Rather, this microgliosis may be due to the effect of Ang II on neurons, which then recruits microglia to the area via paracrine activity, where they subsequently increase neuroinflammation via the secretion of cytokines. The fact that our previous studies indicated that AT1aRs in the PVN are not localized to preautonomic neurons but rather to neuroendocrine cells [36] adds another layer of complexity to the cellular mechanisms by which Ang II causes neuroinflammation. There are at least two possible mechanisms for this effect: (1) that Ang II acts directly in the PVN to influence the neuroendocrine cells, leading to neuroinflammation that influences preautonomic neurons via local paracrine activity, (2) or that AT1R-containing neuroendocrine cells influence preautonomic neurons via local neuronal circuitry, with the subsequent secretion of chemokines that influence microglial migration and activation.

Despite our novel findings, multiple questions and avenues for further research remain. For example, concerning the cellular distributions of AT1aR and AT2R, we have not used the corresponding reporter mice to evaluate their presence on cerebral vessels. Along the same lines of our findings on the cellular location of AT1aR, our current in vivo data indicating that these receptors are located exclusively on neurons in the PVN of the AT1aR-tdTomato reporter mouse strain are in conflict with two previous studies that suggested the presence of AT1R on astrocytes and microglia at this hypothalamic nucleus [83, 84]. In those studies, Percoll density gradients were used to isolate either astrocytes from PVN punches or microglia from the macrodissected hypothalamus, following which the presence of AT1R in the isolated cells was confirmed by RT-PCR [83, 84]. However, it is extremely difficult to dissect *only* the hypothalamus (or indeed the PVN) with such isolation procedures, and the isolates used in the above studies may thus have contained glia from brain tissue surrounding the hypothalamus. The presence of AT1R on glia in these surrounding tissues might explain the discrepancy between our current findings and the findings of these previous studies. Thus, our future studies will include a more detailed investigation of whether AT1Rs are present on astrocytes and microglia in other areas throughout the AT1aR-tdTomato reporter mouse brain. This is warranted as most, but not all, studies using brain cell cultures prepared from whole brain or large brain areas have suggested the presence of functional AT1Rs on glia [85–91].

In summary, the AT1aR reporter, AT2R reporter, and AT1aR/AT2R dual-reporter mice used in this study have provided essential neuroanatomical information on the cellular location of angiotensin receptor subtypes in the brain under normal and diseased (resistant hypertension) conditions. As such, they lay the foundation for further anatomical studies to identify the phenotypes of neurons that harbor AT1aR and AT2R and can also be used for functional (optogenetic) approaches to identify the roles of specific AT1aR- and AT2R-containing neuron populations in cardiovascular and fluid homeostasis and neuroendocrine control under normal and disease states.

Acknowledgements This work was supported by AHA grant 17GRNT33660969 and NIH grants HL-125805 (ADdK), HL-145028 (ADdK), HL-093186 (CS), HL-136595 (EGK/CS), HL-096830 (EGK), and HL-122494 (EGK).

Compliance with ethical standards

Conflict of interest The authors declare that they have no conflict of interest.

Ethical approval All applicable international, national, and/or institutional guidelines for the care and use of animals were followed. Animal procedures were approved by the Institutional Animal Care and Use Committee at the University of Florida, complied with the National Institutes of Health guidelines and were performed in accordance with the Guide for the Care and Use of Laboratory Animals (eight edition, 2011, published by National Academics Press, 500 Fifth Street NW, Washington, DC, 20001, USA) (AALAC #: 000023; OLAW Assurance #: A3377-01).

Animals were housed in temperature- and humidity-controlled rooms on a 12:12 h light/dark cycle with food and water available ad libitum.

References

1. Hollenberg NK. The renin-angiotensin system and sodium homeostasis. J Cardiovasc Pharm. 1984;6 Suppl :S176–183.
2. Dzau VJ. Circulating versus local renin-angiotensin system in cardiovascular homeostasis. Circulation. 1988;77:I4–13.
3. Fitzsimons JT. Angiotensin, thirst, and sodium appetite. Physiol Rev. 1998;78:583–686.
4. Ferguson AV. Angiotensinergic regulation of autonomic and neuroendocrine outputs: critical roles for the subfornical organ and paraventricular nucleus. Neuroendocrinology. 2009;89:370–6.
5. McKinley MJ, Allen AM, Mathai ML, May C, McAllen RM, Oldfield BJ, et al. Brain angiotensin and body fluid homeostasis. Jpn J Physiol. 2001;51:281–9.
6. Miller AJ, Arnold AC. The renin-angiotensin system in cardiovascular autonomic control: recent developments and clinical implications. Clin Auton Res. 2019;29:231–43.
7. Leenen FH. Actions of circulating angiotensin II and aldosterone in the brain contributing to hypertension. Am J Hypertens. 2014;27:1024–32.

8. Marc Y, Llorens-Cortes C. The role of the brain renin-angiotensin system in hypertension: implications for new treatment. Prog Neurobiol. 2011;95:89–103.
9. Young CN, Davisson RL. Angiotensin-ii, the brain, and hypertension: an update. Hypertension. 2015;66:920–6.
10. Lenkei Z, Palkovits M, Corvol P, Llorens-Cortès C. Expression of angiotensin type-1 (at1) and type-2 (at2) receptor mrnas in the adult rat brain: a functional neuroanatomical review. Front Neuroendocrinol. 1997;18:383.
11. Millan MA, Jacobowitz DM, Aguilera G, Catt KJ. Differential distribution of at1 and at2 angiotensin II receptor subtypes in the rat brain during development. Proc Natl Acad Sci USA. 1991;88:11440–4.
12. Tsutsumi K, Saavedra JM. Characterization and development of angiotensin II receptor subtypes (at1 and at2) in rat brain. Am J Physiol. 1991;261:R209-216.
13. Carter DA, Choong YT, Connelly AA, Bassi JK, Hunter NO, Thongsepee N, et al. Functional and neurochemical characterization of angiotensin type 1a receptor-expressing neurons in the nucleus of the solitary tract of the mouse. Am J Physiol Regul. 2017;313:R438–49.
14. Chen D, Jancovski N, Bassi JK, Nguyen-Huu TP, Choong YT, Palma-Rigo K, et al. Angiotensin type 1a receptors in c1 neurons of the rostral ventrolateral medulla modulate the pressor response to aversive stress. J Neurosci. 2012;32:2051–61.
15. Gonzalez AD, Wang G, Waters EM, Gonzales KL, Speth RC, Van Kempen TA, et al. Distribution of angiotensin type 1a receptor-containing cells in the brains of bacterial artificial chromosome transgenic mice. Neuroscience. 2012;226:489–509.
16. de Kloet AD, Wang L, Ludin JA, Smith JA, Pioquinto DJ, Hiller H, et al. Reporter mouse strain provides a novel look at angiotensin type-2 receptor distribution in the central nervous system. Brain Struct Funct. 2016;221:891–912.
17. Brouwers S, Smolders I, Wainford RD, Dupont AG. Hypotensive and sympathoinhibitory responses to selective central at2 receptor stimulation in spontaneously hypertensive rats. Clin Sci. 2015;129:81–92.
18. Dai SY, Peng W, Zhang YP, Li JD, Shen Y, Sun XF. Brain endogenous angiotensin II receptor type 2 (at2-r) protects against doca/salt-induced hypertension in female rats. J Neuroinflammation. 2015;12:47.
19. de Kloet AD, Steckelings UM, Sumners C. Protective angiotensin type 2 receptors in the brain and hypertension. Curr Hypertens Rep. 2017;19:46.
20. Gao J, Zhang H, Le KD, Chao J, Gao L. Activation of central angiotensin type 2 receptors suppresses norepinephrine excretion and blood pressure in conscious rats. Am J Hypertens. 2011;24:724–30.
21. Gao L, Wang W, Li H, Sumners C, Zucker IH. Effects of angiotensin type 2 receptor overexpression in the rostral ventrolateral medulla on blood pressure and urine excretion in normal rats. Hypertension. 2008;51:521–7.
22. Dai SY, Zhang YP, Peng W, Shen Y, He JJ. Central infusion of angiotensin II type 2 receptor agonist compound 21 attenuates doca/nacl-induced hypertension in female rats. Oxid Med Cell Longev. 2016;2016:3981790.
23. Blanch GT, Freiria-Oliveira AH, Speretta GF, Carrera EJ, Li H, Speth RC, et al. Increased expression of angiotensin II type 2 receptors in the solitary-vagal complex blunts renovascular hypertension. Hypertension. 2014;64:777–83.
24. Gao J, Zucker IH, Gao L. Activation of central angiotensin type 2 receptors by compound 21 improves arterial baroreflex sensitivity in rats with heart failure. Am J Hypertens. 2014;27:1248–56.
25. Gao L, Zucker IH. At2 receptor signaling and sympathetic regulation. Curr Opin Pharmacol. 2011;11:124–30.
26. Legat L, Smolders I, Dupont AG. Gabaergic signaling mediates central cardiovascular angiotensin II type 2 receptor effects. Trends Endocrinol Metab. 2018;29:605–6.
27. Ruchaya PJ, Speretta GF, Blanch GT, Li H, Sumners C, Menani JV, et al. Overexpression of at2r in the solitary-vagal complex improves baroreflex in the spontaneously hypertensive rat. Neuropeptides. 2016;60:29–36.
28. Speretta GF, Ruchaya PJ, Delbin MA, Melo MR, Li H, Menani JV, et al. Importance of at1 and at2 receptors in the nucleus of the solitary tract in cardiovascular responses induced by a high-fat diet. Hypertens Res. 2019;42:439–49.
29. Steckelings UM, Kloet A, Sumners C. Centrally mediated cardiovascular actions of the angiotensin II type 2 receptor. Trends Endocrinol Metab. 2017;28:684–93.
30. Han C, Rice MW, Cai D. Neuroinflammatory and autonomic mechanisms in diabetes and hypertension. Am J Physiol Endocrinol Metab. 2016;311:E32–41.
31. Montaniel KR, Harrison DG. Is hypertension a bone marrow disease? Circulation. 2016;134:1369–72.
32. Santisteban MM, Zubcevic J, Baekey DM, Raizada MK. Dysfunctional brain-bone marrow communication: a paradigm shift in the pathophysiology of hypertension. Curr Hypertens Rep. 2013;15:377–89.
33. Farina C, Aloisi F, Meinl E. Astrocytes are active players in cerebral innate immunity. Trends Immunol. 2007;28:138–45.
34. Norris GT, Kipnis J. Immune cells and cns physiology: microglia and beyond. J Exp Med. 2019;216:60–70.
35. de Kloet AD, Pitra S, Wang L, Hiller H, Pioquinto DJ, Smith JA, et al. Angiotensin type-2 receptors influence the activity of vasopressin neurons in the paraventricular nucleus of the hypothalamus in male mice. Endocrinology. 2016;157:3167–80.
36. de Kloet AD, Wang L, Pitra S, Hiller H, Smith JA, Tan Y, et al. A unique "angiotensin-sensitive" neuronal population coordinates neuroendocrine, cardiovascular, and behavioral responses to stress. J Neurosci. 2017;37:3478–90.
37. Grobe JL, Buehrer BA, Hilzendeger AM, Liu X, Davis DR, Xu D, et al. Angiotensinergic signaling in the brain mediates metabolic effects of deoxycorticosterone (doca)-salt in c57 mice. Hypertension. 2011;57:600–7.
38. Hilzendeger AM, Cassell MD, Davis DR, Stauss HM, Mark AL, Grobe JL, et al. Angiotensin type 1a receptors in the subfornical organ are required for deoxycorticosterone acetate-salt hypertension. Hypertension. 2013;61:716–22.
39. Jessberger S, Toni N, Clemenson GD Jr., Ray J, Gage FH. Directed differentiation of hippocampal stem/progenitor cells in the adult brain. Nat Neurosci. 2008;11:888–93.
40. Krause EG, de Kloet AD, Scott KA, Flak JN, Jones K, Smeltzer MD, et al. Blood-borne angiotensin II acts in the brain to influence behavioral and endocrine responses to psychogenic stress. J Neurosci. 2011;31:15009–15.
41. de Kloet AD, Pioquinto DJ, Nguyen D, Wang L, Smith JA, Hiller H, et al. Obesity induces neuroinflammation mediated by altered expression of the renin-angiotensin system in mouse forebrain nuclei. Physiol Behav. 2014;136:31–8.
42. Langlet F, Mullier A, Bouret SG, Prevot V, Dehouck B. Tanycyte-like cells form a blood–cerebrospinal fluid barrier in the circumventricular organs of the mouse brain. J Comp Neurol. 2013;521:3389–405.
43. Kádár A, Sánchez E, Wittmann G, Singru PS, Füzesi T, Marsili A, et al. Distribution of hypophysiotropic thyrotropin-releasing hormone (trh)-synthesizing neurons in the hypothalamic paraventricular nucleus of the mouse. J Comp Neurol. 2010;518:3948–61.
44. Gautron L, Rutkowski JM, Burton MD, Wei W, Wan Y, Elmquist JK. Neuronal and nonneuronal cholinergic structures in the mouse gastrointestinal tract and spleen. J Comp Neurol. 2013;521:3741–67.

45. Mousa SA, Shaqura M, Schäper J, Treskatsch S, Habazettl H, Schäfer M, et al. Developmental expression of δ-opioid receptors during maturation of the parasympathetic, sympathetic, and sensory innervations of the neonatal heart: early targets for opioid regulation of autonomic control. J Comp Neurol. 2011;519:957–71.
46. Liu M, Shi P, Sumners C. Direct anti-inflammatory effects of angiotensin-(1-7) on microglia. J Neurochem. 2016;136:163–71.
47. Mecca AP, Regenhardt RW, O'Connor TE, Joseph JP, Raizada MK, Katovich MJ, et al. Cerebroprotection by angiotensin-(1-7) in endothelin-1-induced ischaemic stroke. Exp Physiol. 2011;96:1084–96.
48. Regenhardt RW, Mecca AP, Desland F, Ritucci-Chinni PF, Ludin JA, Greenstein D, et al. Centrally administered angiotensin-(1-7) increases the survival of stroke-prone spontaneously hypertensive rats. Exp Physiol. 2014;99:442–53.
49. de Kloet AD, Wang L, Pitra S, Hiller H, Smith JA, Tan Y, et al. A unique 'angiotensin sensitive' neuronal population coordinates neuroendocrine, cardiovascular and behavioral responses to stress. J Neurosci. 2017;37:3478–90.
50. Franklin KBJ, Paxinos G. The mouse brain: in stereotaxic coordinates. New York, NY: Elsevier; 2008.
51. Paxinos G, Watson C. The rat brain in stereotaxic coordinates. 7th Edition, Academic Press, San Diego, CA: Elsevier Life Sciences; 2013.
52. Karnik SS, Unal H, Kemp JR, Tirupula KC, Eguchi S, Vanderheyden PM, et al. International union of basic and clinical pharmacology. Xcix. Angiotensin receptors: interpreters of pathophysiological angiotensinergic stimuli [corrected]. Pharmacol Rev. 2015;67:754–819.
53. Shi P, Diez-Freire C, Jun JY, Qi Y, Katovich MJ, Li Q, et al. Brain microglial cytokines in neurogenic hypertension. Hypertension. 2010;56:297–303.
54. Coote JH, Yang Z, Pyner S, Deering J. Control of sympathetic outflows by the hypothalamic paraventricular nucleus. Clin Exp Pharmacol Physiol. 1998;25:461–3.
55. Ciriello J, Kline RL, Zhang TX, Caverson MM. Lesions of the paraventricular nucleus alter the development of spontaneous hypertension in the rat. Brain Res. 1984;310:355–9.
56. Nakata T, Takeda K, Itho H, Hirata M, Kawasaki S, Hayashi J, et al. Paraventricular nucleus lesions attenuate the development of hypertension in doca/salt-treated rats. Am J Hypertens. 1989;2:625–30.
57. Gutkind JS, Kurihara M, Castren E, Saavedra JM. Increased concentration of angiotensin II binding sites in selected brain areas of spontaneously hypertensive rats. J hypertens. 1988;6:79–84.
58. Lenkei Z, Corvol P, Llorens-Cortes C. Comparative expression of vasopressin and angiotensin type-1 receptor mrna in rat hypothalamic nuclei: a double in situ hybridization study. brain Res Mol brain Res. 1995;34:135–42.
59. Santisteban MM, Ahmari N, Carvajal JM, Zingler MB, Qi Y, Kim S, et al. Involvement of bone marrow cells and neuroinflammation in hypertension. Circ Res. 2015;117:178–91.
60. de Kloet AD, Pati D, Wang L, Hiller H, Sumners C, Frazier CJ, et al. Angiotensin type 1a receptors in the paraventricular nucleus of the hypothalamus protect against diet-induced obesity. J Neurosci. 2013;33:4825–33.
61. Obermuller N, Unger T, Culman J, Gohlke P, de Gasparo M, Bottari SP. Distribution of angiotensin II receptor subtypes in rat brain nuclei. Neurosci Lett. 1991;132:11–15.
62. Daniels D. Diverse roles of angiotensin receptor intracellular signaling pathways in the control of water and salt intake. In: De Luca LA, Jr., Menani JV, Johnson AK, editors. Neurobiology of body fluid homeostasis: transduction and integration. Boca Raton, FL: CRC Press/Taylor & Francis; 2014.
63. Ferguson AV, Bains JS. Actions of angiotensin in the subfornical organ and area postrema: implications for long term control of autonomic output. Clin Exp Pharmacol Physiol. 1997;24:96–101.
64. McKinley MJ, McAllen RM, Pennington GL, Smardencas A, Weisinger RS, Oldfield BJ. Physiological actions of angiotensin II mediated by at1 and at2 receptors in the brain. Clin Exp Pharm Physiol Suppl. 1996;3:S99–104.
65. Vieira AA, Nahey DB, Collister JP. Role of the organum vasculosum of the lamina terminalis for the chronic cardiovascular effects produced by endogenous and exogenous ang ii in conscious rats. Am J Physiol Regul. 2010;299:R1564–71.
66. Aguilera G, Young WS, Kiss A, Bathia A. Direct regulation of hypothalamic corticotropin-releasing-hormone neurons by angiotensin-ii. Neuroendocrinology. 1995;61:437–44.
67. Bains JS, Ferguson AV. Paraventricular nucleus neurons projecting to the spinal cord receive excitatory input from the subfornical organ. Am J Physiol. 1995;268:R625–33.
68. Zhu GQ, Patel KP, Zucker IH, Wang W. Microinjection of ang ii into paraventricular nucleus enhances cardiac sympathetic afferent reflex in rats. Am J Physiol Heart Circ Physiol. 2002;282:H2039–2045.
69. Cunningham JT, Beltz T, Johnson RF, Johnson AK. The effects of ibotenate lesions of the median preoptic nucleus on experimentally-induced and circadian drinking behavior in rats. Brain Res. 1992;580:325–30.
70. McKinley MJ, Yao ST, Uschakov A, McAllen RM, Rundgren M, Martelli D. The median preoptic nucleus: front and centre for the regulation of body fluid, sodium, temperature, sleep and cardiovascular homeostasis. Acta Physiol. 2015;214:8–32.
71. Abegaz B, Davern PJ, Jackson KL, Nguyen-Huu TP, Bassi JK, Connelly A, et al. Cardiovascular role of angiotensin type 1a receptors in the nucleus of the solitary tract of mice. Cardiovascular Res. 2013;100:181–91.
72. Colombari E, Colombari DS. Nts at 1a receptor on long-term arterial pressure regulation: putative mechanism. Cardiovasc Res. 2013;100:173–4.
73. Hasser EM, Cunningham JT, Sullivan MJ, Curtis KS, Blaine EH, Hay M. Area postrema and sympathetic nervous system effects of vasopressin and angiotensin ii. Clin Exp Pharmacol Physiol. 2000;27:432–6.
74. Nahey DB, Collister JP. Ang ii-induced hypertension and the role of the area postrema during normal and increased dietary salt. Am J Physiol Heart Circ Physiol. 2007;292:H694–700.
75. Oldfield BJ, Davern PJ, Giles ME, Allen AM, Badoer E, McKinley MJ. Efferent neural projections of angiotensin receptor (at1) expressing neurones in the hypothalamic paraventricular nucleus of the rat. J Neuroendocrinol. 2001;13:139–46.
76. Rowe BP, Saylor DL, Speth RC. Analysis of angiotensin II receptor subtypes in individual rat brain nuclei. Neuroendocrinology. 1992;55:563–73.
77. MacGregor DP, Murone C, Song K, Allen AM, Paxinos G, Mendelsohn FA. Angiotensin II receptor subtypes in the human central nervous system. Brain Res. 1995;675:231–40.
78. Song K, Allen AM, Paxinos G, Mendelsohn FA. Mapping of angiotensin II receptor subtype heterogeneity in rat brain. J Comp Neurol. 1992;316:467–84.
79. Guimond MO, Gallo-Payet N. The angiotensin II type 2 receptor in brain functions: an update. Int J Hypertens. 2012;2012:351758.
80. Lenkei Z, Palkovits M, Corvol P, Llorens-Cortes C. Distribution of angiotensin II type-2 receptor (at2) mrna expression in the adult rat brain. J Comp Neurol. 1996;373:322–39.
81. Haspula D, Clark MA. Neuroinflammation and sympathetic overactivity: mechanisms and implications in hypertension. Auton Neurosci. 2018;210:10–17.

82. Santisteban MM, Kim S, Pepine CJ, Raizada MK. Brain-gut-bone marrow axis: implications for hypertension and related therapeutics. Circ Res. 2016;118:1327–36.
83. Biancardi VC, Stranahan AM, Krause EG, de Kloet AD, Stern JE. Cross talk between at1 receptors and toll-like receptor 4 in microglia contributes to angiotensin ii-derived ros production in the hypothalamic paraventricular nucleus. Am J Physiol Heart Circ Physiol. 2016;310:H404–415.
84. Stern JE, Son S, Biancardi VC, Zheng H, Sharma N, Patel KP. Astrocytes contribute to angiotensin II stimulation of hypothalamic neuronal activity and sympathetic outflow. Hypertension. 2016;68:1483–93.
85. Joglar B, Rodriguez-Pallares J, Rodriguez-Perez AI, Rey P, Guerra MJ, Labandeira-Garcia JL. The inflammatory response in the mptp model of parkinson's disease is mediated by brain angiotensin: relevance to progression of the disease. J Neurochem. 2009;109:656–69.
86. Lanz TV, Ding Z, Ho PP, Luo J, Agrawal AN, Srinagesh H, et al. Angiotensin II sustains brain inflammation in mice via tgf-beta. J Clin Investig. 2010;120:2782–94.
87. Negussie S, Lymperopoulos A, Clark MA. Role of betaarrestin1 in at1 r-mediated mitogen-activated protein kinase activation in wistar and shr brainstem astrocytes. J Neurochem. 2019;148:46–62.
88. Sumners C, Tang W, Zelezna B, Raizada MK. Angiotensin II receptor subtypes are coupled with distinct signal-transduction mechanisms in neurons and astrocytes from rat brain. Proc Natl Acad Sci USA. 1991;88:7567–71.
89. Tallant EA, Higson JT. Angiotensin II activates distinct signal transduction pathways in astrocytes isolated from neonatal rat brain. Glia. 1997;19:333–42.
90. Wu CY, Zha H, Xia QQ, Yuan Y, Liang XY, Li JH, et al. Expression of angiotensin II and its receptors in activated microglia in experimentally induced cerebral ischemia in the adult rats. Mol Cell Biochem. 2013;382:47–58.
91. O'Callaghan EL, Bassi JK, Porrello ER, Delbridge LM, Thomas WG, Allen AM. Regulation of angiotensinogen by angiotensin II in mouse primary astrocyte cultures. J Neurochem. 2011;119:18–26.